Lawrence Berkeley Laboratory
UNIVERSITY OF CALIFORNIA

APPLIED SCIENCE DIVISION

Presented at the Fall Meeting of the
Western States Section/Combustion Institute,
Tucson, AZ, October 27-28, 1986

IGNITION BY EXCIMER LASER PHOTOLYSIS OF OZONE

D. Lucas, D. Dunn-Rankin, K. Hom, and N.J. Brown

October 1986

APPLIED SCIENCE
DIVISION

Prepared for the U.S. Department of Energy under Contract DE-AC03-76SF00098

DISCLAIMER

WSS-86-36

LBL-20871

Ignition by Excimer Laser Photolysis of Ozone

Donald Lucas, Derek Dunn-Rankin*, Kenneth Hom, and Nancy J. Brown

Applied Science Division
Lawrence Berkeley Laboratory
University of California
Berkeley, CA 94720

Fall Meeting
Western States Section/Combustion Institute
Tucson, AZ

Oct. 27-28, 1986

* Present address: Combustion Research Facility, Sandia National Laboratory, Livermore, CA 94550

This work was supported by the Director, Office of Energy Research, Office of Basic Energy Sciences, Chemical Sciences Division of the U. S. Department of Energy under Contract No. DE-AC-03-76SF00098.

ABSTRACT

We have ignited mixtures of hydrogen, oxygen, and ozone in closed cells with 248 nm radiation from a KrF excimer laser. Ozone, the only significant absorber in this system, absorbs a single photon and produces oxygen atoms which initiate combustion. A discretized, time-dependent Beer's law model is used to demonstrate that the radical concentration immediately after photolysis is a function of laser power, ozone concentration, focal length, and separation between the lens and reaction cell. Spark schlieren photographs are used to visualize the ignition events and identify the ignition sites. The effects of equivalence ratio, pressure, and the initial gas temperature on the minimum ozone concentration needed to produce ignition are presented, and only the initial temperature has a significant effect. Modelling studies of the ignition process aid in the interpretation of the experimental results, and show that the ignition we observe is not due solely to thermal effects, but is strongly dependent on the number and type of radicals present initially after photolysis. Ignition using other hydrocarbons as fuels was also demonstrated.

In this paper, we describe a study of ignition initiated by ozone photolysis at 248 nm by radiation from a KrF excimer laser. We use a discretized, time-dependent absorption model to predict the spatial dependence of the oxygen atoms produced by photolysis, and model the H_2/O_2 kinetics to evaluate the relative importance of thermal and chemical energy addition. We also compare locations of the calculated maximum concentration with observed ignition sites to show that simple photolysis is responsible for the production of oxygen atoms, and that the ignition is dependent on both the concentration of radicals produced initially as well as the size of the ignition site.

PHOTOCHEMISTRY REVIEW

The absorption spectrum of ozone exhibits continuous absorption throughout the visible and ultraviolet, with the strongest absorption occurring in the Hartley band near 255 nm, where $\varepsilon = 130\ cm^{-1}atm^{-1}$. Absorption in this band places ozone in the dissociative (S_1) state, with a quantum yield for oxygen atoms of essentially unity[16]. Decomposition of the ozone into O_2 and O is energetically possible at wavelengths below 1190 nm, as the bond energy is 100.0 kJ/mole[16]. Several researchers[17-22] have measured the product distribution for ozone photolysis at 248 nm, and have found that approximately 10% of the oxygen molecules is in the ($^3\Sigma_g^-$) ground state with the oxygen atoms in the (^3P) state. The other 90% is in a Boltzmann distribution in the vibrational states of the ($^1\Delta$) electronic state for O_2, with the oxygen atoms in the (^1D) state.

The choice of ozone as the absorber in this study was based in part on the assumption that photolysis at 248 nm would be a single photon event. Readers may question this assumption in light of the

high laser power employed in this study; therefore the experimental evidence that indicates that no multiphoton effects are present in our system is reviewed in the next paragraph.

The bulk of the experimental evidence comes from the work of Lee and co-workers[17-20], who studied the interaction of ozone molecules with laser radiation in the collision-free regime of a supersonic molecular beam. Analysis of the angular distribution of the ozone photofragments indicates that dissociation can be viewed as being impulsive, occurring in less than one vibrational period (approximately 10^{-13} sec)[18]. The highly dissociative S_1 upper electronic state of ozone greatly reduces the possibility of any significant two photon interactions even with the high energy laser used in this study. Additional conclusive evidence is found in the measurement of the energy distribution in the fragments[17,19]. At both 266 and 248 nm the sum of the energy in the O and O_2 fragments plus the ozone bond energy <u>never</u> exceeds the energy contained in a single photon. It is important to note that the energy densities used in the studies of Lee and co-workers are similar to those employed in this study. They also found no evidence for increased absorption in ozone as the laser power was increased (as would be expected for a multiphoton event) to levels in excess of 200 mJ/cm^2- higher levels than in our unfocussed beam ignition experiments. Even more tightly focussed beams did not produce multiphoton absorption[20].

No other species present during the laser pulse has a significant absorption at 248 nm. Oxygen has an absorption coefficient of less than 0.005 cm^{-1} atm^{-1}, four orders of magnitude below that for ozone, and light at this wavelength is not sufficient to produce atomic

oxygen (the threshold is 242.2 nm)[16]. The absorption spectrum of excited oxygen ($^1\Delta$) is assumed to be similar in shape to the ground state molecule, shifted by approximately 94 kJ/mole to the red. This would place the absorption maximum near 157 nm, still far from the laser wavelength of 248 nm.

Excited oxygen atoms are very reactive, with the (^1D) state lying 190.0 kJ/mole above the (^3P) ground state. Oxygen (^1D) reacts with H_2 with zero activation energy, and a rate coefficient of 1×10^{-10} cm^3 $molec^{-1}$ sec^{-1}, producing OH and H as products, and releasing 182.1 kJ/mole (at 298 K). Quenching rates with H_2 are slower than reaction by a factor of 40 [23].

Little is known about the reactions of the metastable oxygen molecule, $O_2(^1\Delta)$. The energy of this state is 94.2 kJ/mole above the ground state, and its radiative lifetime is on the order of 64 min. Some O_2 ($^1\Delta$) quenching rates for species of interest in this study are 2×10^{-18} for O_2, 5.3×10^{-18} for H_2, and 4.4×10^{-15} for O_3 (cm^3 $molec^{-1}$ s^{-1} at 300 K)[23].

The reaction conditions after the laser pulse can be reasonably well characterized. The number of oxygen atoms produced in each state by photolysis can be calculated from the experimental conditions as described in the following section, with the excess photon energy appearing as heat. Some energy is contained in excited oxygen molecules and atoms where it remains until reaction. Excited O (^1D) atoms can react or be deactivated, releasing more energy. The total energy released causes a temperature and pressure rise in the gas mixture which can be calculated using the heat capacity of the mixture.

METHOD OF APPROACH

A. Experiment

Krypton fluoride radiation at 248 nm from a Lamda Physik 200EMG excimer laser was used to photolyze ozone/oxygen/fuel mixtures in a constant volume cell. The light was focussed by MgF_2 or UV grade quartz lenses of various focal lengths through windows of the same materials. Laser outputs were measured with a Gentec ED-500 joulemeter, and in typical experiments 350 to 400 mJ of light entered the reaction cell. Two aluminum cells were used; one was 37 x 37 x 118 mm, with Plexiglas side windows for optical access, and the other was a cylinder 30 mm in diameter and 140 mm long which could be heated by an external electrical resistance heater. A schematic diagram of the apparatus is shown in the top portion of Fig. 1.

Gases were obtained from LBL supplies and used without further purification. All gases except ozone were metered using calibrated flow controllers, and mixed in a stainless steel tube packed with pyrex spheres before introduction into the cell. Ozone was produced by passing oxygen through two Thermo Electron ozinators in series, and trapped on silica gel cooled to dry ice-isopropanol temperature. Excess oxygen was removed by pumping before warming the silica gel to room temperature. Ozone concentrations in the reaction cells were monitored immediately before laser photolysis by absorption using a deuterium lamp/monochrometer/photomultiplier assembly. Ozone pressures of up to 60 torr could be obtained, with a purity in excess of 95%.

Initial gas pressures, measured with an MKS baratron, were in the range of 20 to 200 torr. Transient pressure measurements were made with a Kistler 211B piezotron flush mounted in the cell wall. A

DEC/CAMAC microcomputer system described previously[13] controlled timing and recorded the pressure data.

Spark schlieren photography was used to visualize the absorption and combustion events. Photographs were obtained using two 1.0 m focal length lenses and a knife edge stop, arranged in a U shape because of space limitations.

Variation of the ozone partial pressure was the primary method for establishing ignition conditions. Combustion was confirmed by visual observation, pressure rise, and the appearance of water on the cell windows. For a single set of initial conditions up to 20 experiments were conducted to ensure accuracy and reproducibility. The system was quite sensitive to changing the ozone pressure, with a change of less than 4% in the partial pressure of the ozone sufficient to change a no-burn case into a repeatable combustion event.

B. Calculation of Radical Concentration

Photochemical ignition is sensitive to laser power, degree of light focussing, and ozone concentration, with each factor affecting the concentration of radicals available to initiate combustion. Implicit in the usual formulation of Beer's law, Absorbance = εcl, is the assumption that the number of absorbing species is large compared with the number of photons. In high energy laser systems with strongly absorbing species this assumption can be easily violated. We thus used a discretized, time-dependent model to calculate the number of photons absorbed as a function of distance in the illuminated volume.

We temporally separate the laser pulse into photon packets. The number of photons in each packet corresponds to the temporal behavior of the laser pulse specified by the manufacturer. Typically 100 packets are used in the calculations. The beam is assumed to have a uniform spatial energy distribution in accordance with manufacturer's specifications. The initial beam size and energy were measured using a joulemeter, and the beam waist size and location determined utilizing burn spots on Polaroid film. Input variables include the laser power, the focal length of the lens, the distance between the lens and the cell window, and the ozone concentration, all which are measurable quantities.

Calculations begin by determining the area of the beam at a given spatial location. The beam is assumed to be a fixed area rectangle before the lens. After the lens, the rectangle area collapses at a constant rate from the initial size of the laser to that of the measured minimum beam size. Past the focal point the beam is assumed to expand at the same rate that it became focussed. Area expansion due to the divergence of the laser is not included.

The illuminated volume is divided into cells of fixed length, with the length size varied as a parameter. The intensity of a photon packet exiting the first cell is calculated using Beer's law and an absorption coefficient of 120 cm^{-1} atm^{-1}, with this intensity then used as the initial intensity for the next cell. The step size is chosen so that less than half of the light entering a cell is absorbed. Each photon absorbed is assumed to dissociate an ozone molecule, producing one oxygen atom and one oxygen molecule. Recombination reactions which reform ozone during the laser pulse of 17 nsec are considered negligible. Results from each photon packet

are summed to obtain the total oxygen atom concentration in the illuminated volume at a given axial distance in the cell.

C. Kinetic Modelling

Ignition was modelled as homogeneous, constant volume combustion using appropriate species and energy conservation equations. The CHEMKIN code[24] with an appropriate driver routine was used to solve the equations for temperature, pressure, and species concentrations as a function of time. The reactions and rate coefficients used in modelling H_2/O_2 mixtures were those given by Miller et al.[25] with two exceptions. The reaction $O + H_2O_2 \rightarrow OH + HO_2$ was added, and the rate coefficient for this and $O + H_2 \rightarrow H + OH$ were taken from a recent compilation by Warnatz[26]. The kinetic model was checked by reproducing the explosion limits given in Lewis and von Elbe[27] for stoichiometric combustion at several pressures. The temperature thresholds for explosion at a given pressure were reproduced to within 30 K. Induction periods given by Dixon-Lewis and Williams[28] were reproduced to within 20%. Results of these calculations will be presented during discussion of the temperature effects.

RESULTS AND DISCUSSION

1. Radical Concentration

Results of the radical concentration calculations (Sec. A above) for the range of conditions employed in the experiments are shown in Figs. 2 - 5. Experimentally measured values of the initial and focussed laser beam size and energy, focal length of the lens, separation of the lens and combustion cell, and ozone concentration are used in the calculations. The abscissa is the distance from the

entrance window of the cell, and the ordinate is the number density of ozone molecules that have absorbed a photon in the volume illuminated by the laser, and is equal to the number of O atoms produced by photolysis. These figures present separately the effect of changing ozone concentration, laser power, focal length of the lens, and separation distance between the cell and the lens while holding all other parameters constant.

The curves illustrate the consequences of two effects- a Beer's law behavior when the number of absorbers is large compared with the number of photons and bleaching when the opposite condition pertains. It should be noted that the cusps appearing in these figures are an artifact of the method used to calculate the beam area. However, because the minimum area size is fixed in the calculations, the concentration at the focus is not significantly affected.

Examination of Fig. 2 indicates that the maximum radical concentration can be either at the focus or the wall, and that an increase in ozone concentration does not necessarily lead to an increase in radical concentration at a given spatial location in the cell. These results suggest ignition experiments where a constant radical concentration is maintained but the size of the ignition site is varied. Figure 3 is evidence that bleaching can be significant with a light source such as a high energy output laser. With bleaching, the concentration of radicals produced does not increase with increasing laser power. As expected, calculations involving various focal lengths, Fig. 4, indicate that ozone absorption follows Beer's law when no lens is used (focal length = infinity). Examination of Figure 5. reveals that simply moving the lens can

result in significant changes in the radical concentration profile.

The calculations can be used to demonstrate that the proper choice of experimental parameters can reduce uncertainties in determining minimum ignition conditions. For example, most excimer lasers outputs vary by 10% on a shot-to-shot basis (our laser was measured to have a standard deviation of 3.53%). However, if the bleaching conditions are met, there is no change in the maximum concentration of radicals produced, and only a small change in the volume in which this concentration exists. Another important observation is that when bleaching occurs, no ozone remains in that volume. This reduces the complexity of the ignition kinetics to that of the fuel, oxygen, and radicals produced by photolysis.

These results suggest that a rather complete knowledge of the experimental conditions is necessary to insure that the maximum concentration of radicals occurs at the desired point, and that a simple Beer's law assumption will not be valid in most cases where a focussing lens is used.

2. Ignition

The minimum ozone concentrations for ignition were measured as a function of equivalence ratio, initial temperature, and type of fuel, with most of the experiments performed using H_2 as the fuel.

A. Ignition Site

We performed experiments to locate the ignition site for a particular set of conditions. These experiments also confirm that the laser energy density is not the crucial factor that determines whether or not ignition occurs, but rather it is the concentration of radicals produced by single photon absorption. This is significant because single photon absorption provides a reasonably simple means of

determining the number of molecules that absorb a photon, which is difficult to assess when multiphoton effects are present.

Schlieren photographs of the ignition events are shown in Figs. 1 and 6, with each photograph taken during a separate experiment. The ozone concentration was varied, and the H_2/O_2 ratio and the initial pressure were held constant. Changing the ozone concentration over the range employed in this study did not significantly alter the equivalence ratio. The top photograph in Fig. 1 was recorded 5 microseconds after the laser fired. The ozone pressure for this case was 7.0 torr, and the mixture eventually burned. A sharp outline due to the temperature gradient produced by the absorption of light by ozone is observed, as well as a weak shock front which propagates perpendicular to the direction of laser travel. This shock wave is observed to travel at approximately the speed of sound for this mixture, and cannot be distinguished after approximately 20 microseconds. The lower photograph in Fig. 1 is for a 5.5 torr ozone pressure 200 microseconds after laser firing. No combustion was observed for this mixture, but the schlieren image is broader and less distinct because of diffusion and thermal transport effects. We observe no significant differences in the schlieren images between igniting and non-igniting cases at times less than 5 microseconds.

The top two images in Fig. 6 were taken with an initial ozone pressure of 5.7 torr. Ignition occurs near the focus, and the ignition kernel is evident only at times greater than 150 microseconds after the laser pulse. The image in Fig. 6 recorded at 200 microseconds should be compared with the 200 microsecond photograph of the non-igniting case in Fig. 1. The lower two photographs in Fig. 6

were taken with time delays of 25 and 200 microseconds, and an ozone pressure of 9.0 torr. Ignition is clearly evident 25 microseconds after the laser pulse, with burning occurring near the entrance window, and propagating into the cell. Essentially complete combustion is evident by 200 microseconds.

The difference in ignition times and the robustness of the ensuing combustion can be attributed to several factors. When ignition occurs near the focus, only a small kernel is generated compared with ignition near the window. Transport of species and cooling of the kernel are thus much less important for window ignition. Calculations indicate that the ozone is not completely dissociated at the window, and that the initial oxygen atom concentration is 25% higher for this case than when ignition occurs at the focus. Both the increased radical concentration and the presence of unreacted ozone will increase the reaction rate. Countering these effects is cooling of the ignition kernel by the window. However, because ignition occurs in a relatively short time, we expect that this effect is not large.

It is important to emphasize that if multiphoton effects were significant one would expect enhanced ignition at the focus, where the laser intensity is highest. The two ignition sites have laser power densities differing by a factor of 25. If ignition were a result of a multiphoton absorption, the radical and/or ion concentration would depend on at least the second power of the laser intensity or peak power level (a factor of at least 600). These results, in conjunction with the theoretical and experimental evidence presented in the Photochemistry Review section, indicate that only a single photon is absorbed by an ozone molecule, and that there are no

significant multiphoton effects in our system.

Pressure traces recorded during these events are shown in Fig 7. The lower trace, recorded when combustion began near the focus, shows a longer induction time, and a slower pressure rise than the upper trace, which had ignition near the window. The ignition site thus can be correlated with the pressure characteristics, reducing the need to fully document each combustion event with the more laborious photographic method.

B. Equivalence Ratio

Figure 8 shows results from experiments performed at different equivalence ratios. There was no significant difference in the measured amount of ozone needed to initiate combustion for hydrogen/oxygen/ozone mixtures at equivalence ratios between 0.5 and 3.3. Our results should be compared with the experimental results of Lavid and Stevens[14], who found a minimum for photochemical initiation at an equivalence ratio of 0.6, but no significant difference at equivalence ratios of 0.4, 1.0, and 1.6. Guirguis et al.[29], in their computational study of radical enhanced oxidation of methane, found their results invariant at equivalence ratios of 0.5 and 1.0.

C. Temperature Effects and Modelling

The minimum ozone concentrations required for ignition were measured as a function of temperature at an equivalence ratio of 0.55. Raising the gas temperature reduced the ozone mole fraction required from 0.0178 at 300 K, 0.0166 at 330 K, to 0.0147 at 370 K.

Radical concentrations were calculated using the discretized Beer's law model described earlier, and are presented in Fig. 9. For all three sets of experiments the maximum is at the focus, with

complete dissociation of the ozone and nearly identical kernel sizes. Analysis of these results is directed toward acquiring some understanding of the relative roles of thermal and chemical reactivity in promoting combustion. The energy input to the system can be divided between different chemical species (in various states) and heat. The various products arising from ozone photolysis have been described earlier, and we assume rapid relaxation of vibrational and rotational states. We can thus describe the initial conditions in the cell for cases where ignition occurs, and use these results in our kinetic modelling.

The minimum number of radicals needed for ignition in our system initially at 300 K is 1.2×10^{17} cm^{-3}. This should be compared with the results of Lavid and Stevens[14], who calculated that approximately 3×10^{17} cm^{-3} oxygen atoms are necessary in their H_2/O_2 system ignited by 157 nm radiation. We have shown that ozone is bleached from the ignition kernel, so the chemistry of the two systems is similar. There are differences in the photon energy, wall losses, and the fact that our system produces a greater fraction of O atoms in an excited state (90% versus 50%). However, we are encouraged by the close agreement between the two experiments.

For the kinetic modelling calculations, three sets of initial conditions were assumed for the experiments described above. All cases assume that ozone is the only absorbing species, and that the ozone is bleached. The amount of energy deposited in the kernel is determined using the discretized time dependent Beer's law calculation. Case I assumptions are that all of the energy absorbed appears as heat in the ignition kernel, and that no radical species

are present; Case II assumes that the ozone dissociates and produces oxygen atoms and oxygen molecules in their ground state; and Case III assumes that 90% of the ozone dissociation products are in their excited electronic states (O (^1D) and O_2 ($^1\Delta$)), and that the excited oxygen atoms react immediately with H_2 to produce OH and H with the liberation of 181.8 kJ $mole^{-1}$. A temperature, T^e, is calculated for each case using the initial gas temperature, the number and energy of absorbed photons in the kernel, and the heat capacity of the system. The thermal threshold temperature (T^*), the lowest temperature for which ignition occurs, is determined by solving the conservation equation for appropriate conditions of species concentrations and pressure at several input temperatures. These results are presented in Table I.

The threshold temperatures for thermal ignition are significantly higher than those calculated assuming that all the laser energy absorbed appears as heat, thus eliminating Case I as the ignition mechanism. Calculated temperatures (T^e) are close to threshold temperatures for Case II and are lower than those for Case III. These results indicate that the mechanism of ignition occurring in the kernel is intermediate between Cases II and III, and that ignition is strongly dependent on the number and type of radical species produced. Important factors in determining the relative roles of Cases II and III include knowledge of the quenching rates for O (^1D) and O_2 ($^1\Delta$), and the detailed chemistry of both excited species, information that is only partially available.

The modelling results show that introduction of radicals enables chemical reactions to occur, which raises the temperature of the mixture and further accelerates reactions and heat release. However,

the immediate recombination of radicals does not provide sufficient energy to raise the temperature of the mixture above the thermal threshold. This is illustrated by considering calculations in which the initial O_2, H_2, and O atom concentrations are fixed (Case II) and the initial temperature is increased from some low value to the threshold temperature in 10 K increments. Below the threshold, the final temperature of the mixture is not the initial temperature plus some fixed increment. Instead, the increment increases with initial temperature due to the radical initiated chemistry. In contrast, when approaching the threshold temperature for Case I, (no radicals initially present), the chemistry which occurs is insignificant and the final temperature nearly equals the initial temperature. The presence of radicals in the initial mixture also reduces the induction time at threshold by a factor between 10 and 20.

Calculations were also made to assess the effects of pressure and equivalence ratio on the threshold temperatures for Cases I and II. Using Case II conditions for lean mixtures and pressures of 0.4 and 0.5 atm resulted in threshold temperatures of 560 and 550 K, respectively. Thus the variation in pressure caused by the differences in ozone absorption does not significantly affect threshold values. Threshold temperatures for Case I were computed for ϕ = 0.5, 1.0, and 1.5, and a 10 K difference was found between the rich mixture and the others. The threshold temperatures in lean and stoichiometric mixtures for Case II conditions were also within 10 K of each other. The insensitivity of ignition conditions to variations in equivalence ratio over this range concurs with our experimental observations.

D. Pressure Effects

Pressure effects were difficult to determine in our apparatus. Initial pressures greater than 250 torr could not be used without destruction of the windows. Ignition of hydrogen/oxygen was possible at pressures as low as 20 torr, but studies at lower pressure were precluded since there was no dependable means of detecting ignition.

E. Fuel Type

Preliminary experiments were conducted comparing hydrogen, methane, and propane as fuels. To reduce potential multiphoton absorption by the hydrocarbons the laser light was not focussed. Ignition thus occurs at the window, under conditions where the radical concentration is at a maximum, and some undissociated ozone remains in the ignition kernel. The equivalence ratio for all fuels was held at 0.96, and an initial pressure of 80 torr. The hydrogen mixture was the easiest to ignite, requiring an initial ozone pressure of 4.5 torr, compared with propane, which needed 9.8 torr, and methane, which required 15.6 torr. These pressures resulted in an initial oxygen atom concentration of 0.96×10^{17}, 2.0×10^{17}, and 3.2×10^{17} molec cm^{-3}, respectively. Our results can be compared with spontaneous ignition temperatures, and minimum ignition parameters shown in Table II. While it is somewhat difficult to compare the results directly, it is interesting to note that the trends for the different ignition criteria are not in agreement, further proof that the laser ignition we observe is different from both the thermal and spark ignition cases.

CONCLUSION

We have ignited mixtures of hydrogen, oxygen, and ozone in closed cells with 248 nm radiation from a KrF excimer laser. Ozone, the only significant absorber in this system, absorbs a single photon and produces oxygen atoms which initiate combustion. A discretized, time-dependent Beer's law model is used to demonstrate that the radical concentration immediately after photolysis is a function of laser power, ozone concentration, focal length, and separation between the lens and reaction cell. Spark schlieren photographs are used to visualize the ignition events and identify the ignition sites. The effects of equivalence ratio, pressure, and the initial gas temperature on the minimum ozone concentration needed to produce ignition are presented, and only the initial temperature has a significant effect. Modelling studies of the ignition process aid in the interpretation of the experimental results, and show that the ignition we observe is not due solely to thermal effects, but is strongly dependent on the number and type of radicals present initially after photolysis. Ignition using other hydrocarbons as fuels was also demonstrated.

ACKNOWLEDGMENT

We thank A. K. Oppenheim for his generous loan of the excimer laser, D. Littlejohn for helpful advice with the ozone trapping system and use of a UV spectrometer, and O. Rashed for assistance in the computations. This work was supported by the Director, Office of Energy Research, Office of Basic Energy Sciences, Chemical Sciences Division of the U. S. Department of Energy under Contract No. DE-AC-03-76SF00098.

REFERENCES

1. Dale, J. D., Smy, P. R., Way-Nee, D, and Clements, R. M., Combust. Flame 30, 319 (1977).

2. Schmieder, R. W., J. Appl. Phys. 52, 3000 (1981).

3. Miziolek, A. W., Sausa, R. C., BRL Report BRL-TR-2644, Feb., 1985.

4. Trott, W. M., J. Appl. Phys, 54, 118 (1983).

5. Bauer, S. H., Bar-Ziv, E., and Haberman, J. A., IEEE J. Quant. Elect. QE-14, 237 (1978).

6. Avouris, Ph., Bethune, D. S., Lankard, J. R., Ors, J. A., and Sorokin, P. P., J. Chem. Phys. 74, 2304 (1981).

7. Lyman, J. L., and Jensen, R. J., J. Phys. Chem. 77, 883 (1973).

8. Hill, R. A., Appl. Optics 20, 2239 (1981).

9. Hill, R. A., and Laguna, G. A., Optics Comm. 32, 435 (1980).

10. Raffel, B., Warnatz, J., and Wolfrum, J., Appl. Phys. B 37, 189 (1985).

11. Maas, U., Raffel, B., and Wolfrum, J., to be published in the 21st. Symposium (Int.) on Combust.

12. Norrish, R. G. W., 10th Symposium (Int.) on Combust., 1 (1965).

13. Lucas, D., Peterson, R., Brown, N. J., and Oppenheim, A. K., 20th Symposium (Int.) on Combust., 1205 (1985).

14. Lavid, M. and Stevens, J. G., Combust. Flame 60, 195 (1985).

15. Chou, M., and Dean, A. M., to be published in Int. J. Chem. Kin.

16. Calvert, J. G. and Pitts, J. N., Photochemistry, Wiley and Sons, New York (1966).

17. Sparks, R. K., Carlson, L. R., Shobatake, K., Kowalczyk, M. L., and Lee, Y. T., J. Phys. Chem. 72, 1401 (1980).

18. Carlson, L. R., Ph. D. Thesis, University of California, Berkeley (1979).

19. He, G., Sparks, R. J., Kwok, H. S., and Lee, Y. T., MMRD Annual Report, LBL-12000, p. 304, June, 1981.

20. Lee, Y. T., private communication.

21. Amimoto, S. T., Force, A. P., Wiesenfeld, J. R., and Young, R. H., J. Chem Phys. 73, 1244 (1980).

22. Wine, P. H., and Ravishankara, A. R., Chem. Phys. 69, 365 (1982).

23. Okabe, H., Photochemistry of Small Molecules, Wiley-Interscience, New York, N. Y. (1978).

24. Kee, R. J., Miller, J. A., and Jefferson, T. H., CHEMKIN, SAND80-8003, (1980).

25. Miller, J. A., Branch, M. C., McLean, W. J., Chandler, D. W., Smooke, M. D., and Kee, R. J., 20th Symposium (Int.) on Combust., 673 (1985).

26. Warnatz, J., Chap. 5 in Chemistry of Combustion Reactions, Gardiner, W. S., ed., Springer-Verlag, New York, N. Y., (1983).

27. Lewis, B., and von Elbe, G., Combustion, Flames and Explosions of Gases 2nd ed., Academic Press, New York, N. Y., (1961).

28. Dixon-Lewis, G., and Williams, D. J., in Comprehensive Chemical Kinetics, Bamford and Tipper, eds., Elsevier Scientific, Amsterdam, p. 1 (1977).

29. Guirguis, R. H., Oppenheim, A. K., Karasalo, I., and Creighton, J. R., in Combustion in Reactive Systems, Bowen et al., eds, Progress in Astronautics and Aeronautics, Vol. 76 (1981).

30. Kanury, A. M., Introduction to Combustion Phenomena, Gordon and Breach, New York, N. Y., p. 124 (1977).

Table I

Modelled Ignition Temperatures and Estimated Experimental Temperatures

Initial Temperature (K)	Initial Composition	Initial Pressure (atm)	Case	T^e (K)	T^* (K)
300	H_2 = 0.512 O_2 = 0.488	0.468	I	604	885
300	H_2 = 0.5027 O_2 = 0.4794 O = 0.0178	0.50	II	541	560
300	H_2 = 0.4948 O_2 = 0.4719 O = 0.0018 OH = 0.0158 H = 0.0158	0.40	III	474	330
330	H_2 = 0.5040 O_2 = 0.4794 O = 0.0166	0.50	II	577	570
330	H_2 = 0.4965 O_2 = 0.4725 O = 0.0016 OH = 0.0147 H = 0.0147	0.40	III	511	350
370	H_2 = 0.5061 O_2 = 0.4792 O = 0.0147	0.50	II	614	590
370	H_2 = 0.4995 O_2 = 0.4729 O = 0.0014 OH = 0.0130 H = 0.0130	0.40	III	549	370

Table II

Ignition conditions for fuel/oxygen mixtures

Fuel	Photolysis O atom concentrations (atoms/cm3) (a)	Spontaneous Ignition		Emin (μJ) (d)	Dmin (mm) (e)
		Temperature (K) (b)	Energy (kJ) (c)		
H_2	0.96×10^{17}	833	16.1	4.2	0.25
C_3H_8	2.0×10^{17}	741	19.9	4.2	0.24
CH_4	3.2×10^{17}	829	19.4	6.3	0.30

a) This work

b) Ref. 30 Stoichiometric fuel/oxygen at 1.0 atm.

c) Energy needed to raise one mole of stoichiometric mixture to the spontaneous ignition temperature.

d) Minimum spark energy needed for ignition (Ref. 30).

e) Quenching distance for spark ignition (Ref. 30).

FIGURE CAPTIONS

Fig. 1. Schematic of experimental apparatus and spark schlieren photographs revealing laser interaction with ozone. The mixture depicted in the top photograph eventually ignited, while the gas depicted in the bottom photograph did not burn.

Fig. 2. Initial oxygen atom concentration calculated for ozone absorption of 248 nm light as a function of ozone concentration. Default parameters are: ozone concentration = 4.0 torr, laser power = 350 mJ, focal length = 5.0 cm, and lens-window separation = 1.0 cm.

Fig. 3. Initial oxygen atom concentration calculated as a function of laser power. All other parameters are at default values in Fig. 5.

Fig. 4. Initial oxygen atom concentration calculated as a function of focal length. All other parameters are at default values in Fig. 5.

Fig. 5. Initial oxygen atom concentration calculated as a function of lens-window separation. All other parameters are at default values in Fig. 5.

Fig. 6. Spark schlieren photographs of laser ignition in hydrogen/oxygen/ozone mixtures.

Fig. 7. Pressure measurements in laser ignited mixtures of hydrogen/oxygen/ozone. Ignition occurs at the window for top trace, and at the focus for bottom trace. The laser was fired at the time denoted by the arrow.

Fig. 8. Variation in minimum ozone pressure necessary for ignition at different equivalence ratios. The line is added only for clarity. ◊ - no ignition, □ - ignition.

Fig. 9. Initial oxygen atom concentrations calculated from experiments determining the minimum ozone concentration for ignition of hydrogen/oxygen/ozone mixtures at three different initial gas temperatures.

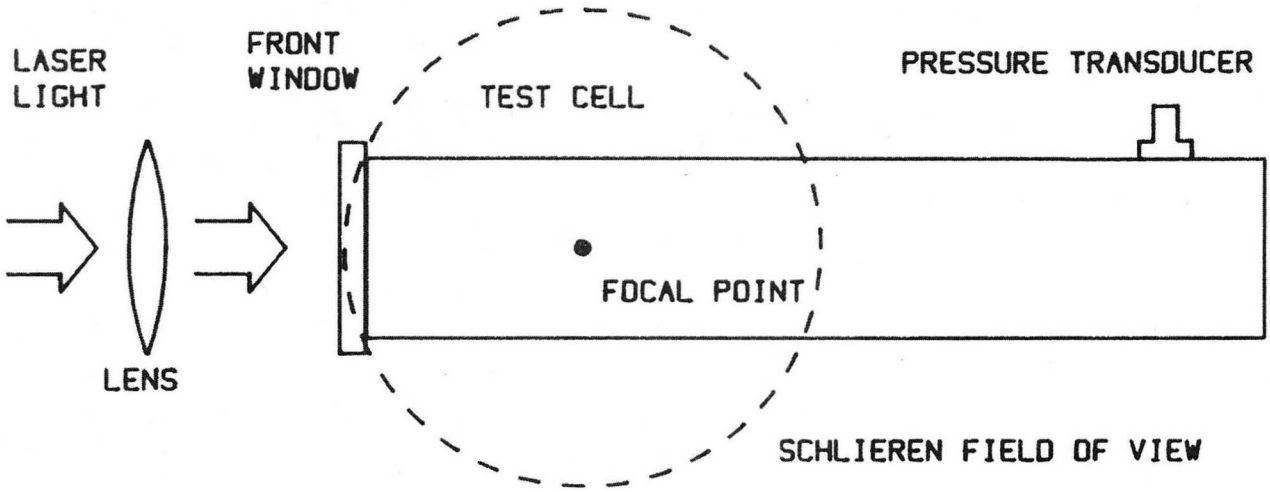

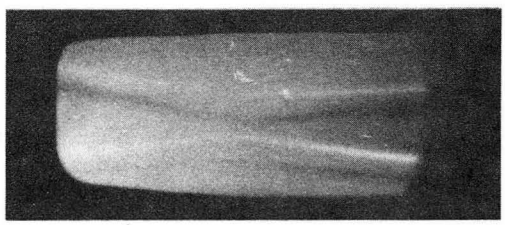

5.0 microseconds

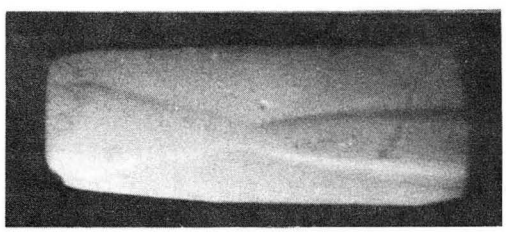

200 microseconds

XBB 861-129

Figure 1.

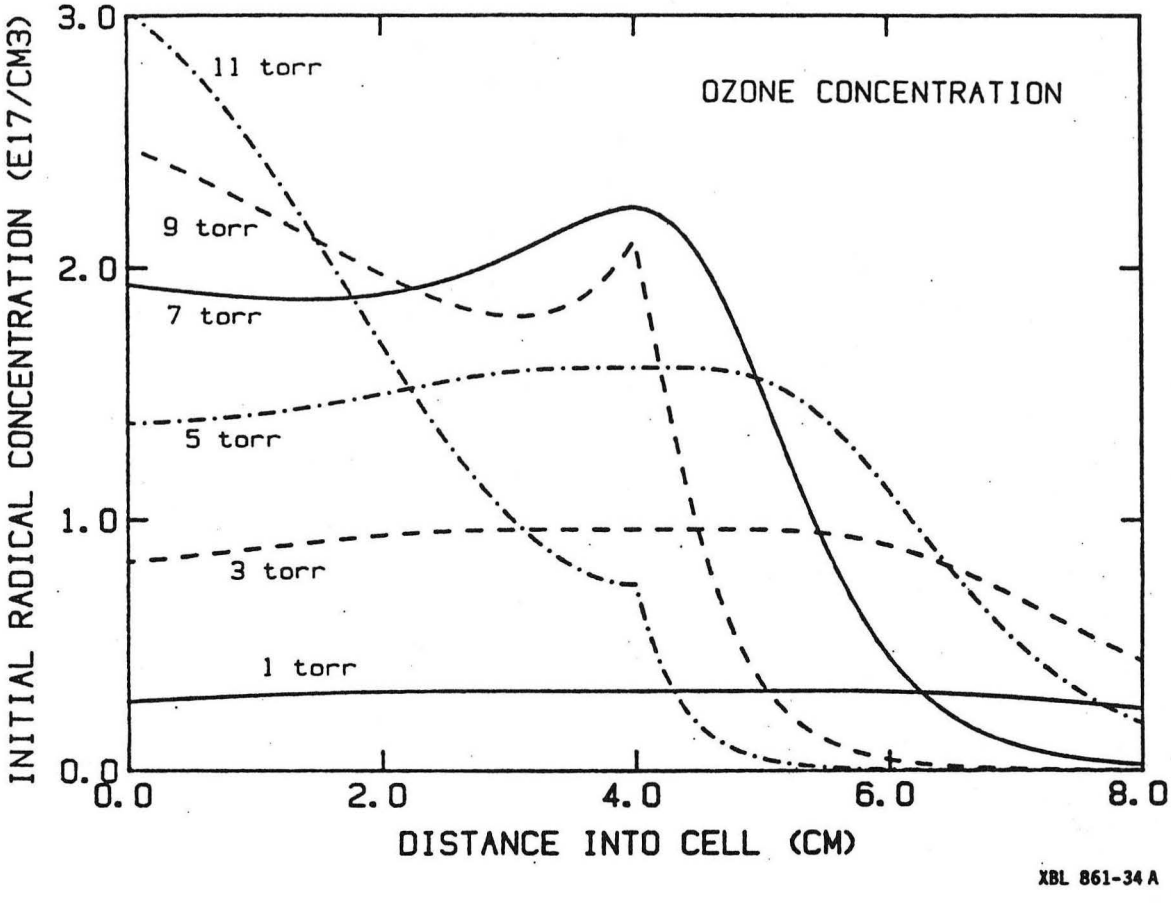
OZONE CONCENTRATION
11 torr
9 torr
7 torr
5 torr
3 torr
1 torr
INITIAL RADICAL CONCENTRATION (E17/CM3)
3.0
2.0
1.0
0.0
0.0
2.0
4.0
6.0
8.0
DISTANCE INTO CELL (CM)
XBL 861-34 A

Figure 2.

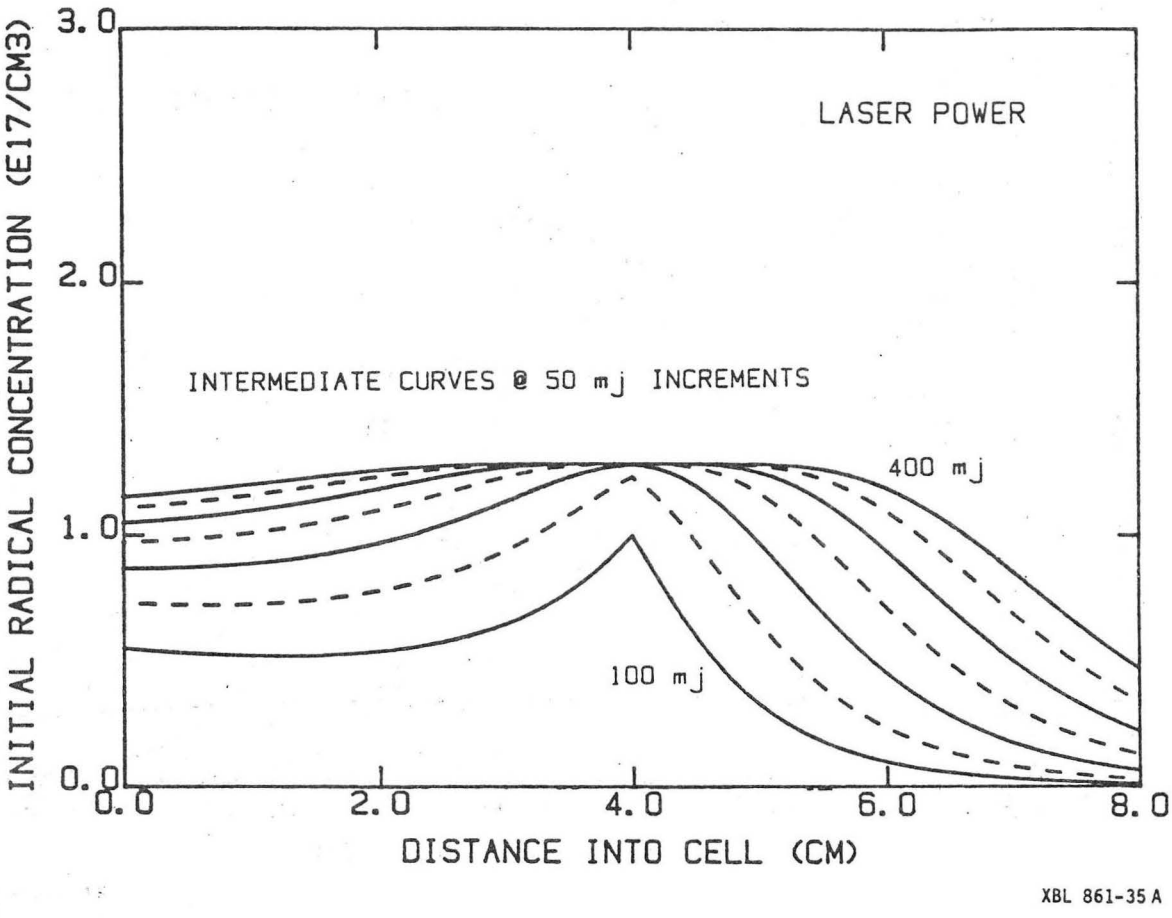
INITIAL RADICAL CONCENTRATION (E17/CM3)
3.0
2.0
1.0
0.0
LASER POWER
INTERMEDIATE CURVES @ 50 mj INCREMENTS
400 mj
100 mj
0.0
2.0
4.0
6.0
8.0
DISTANCE INTO CELL (CM)
XBL 861-35 A

Figure 3.

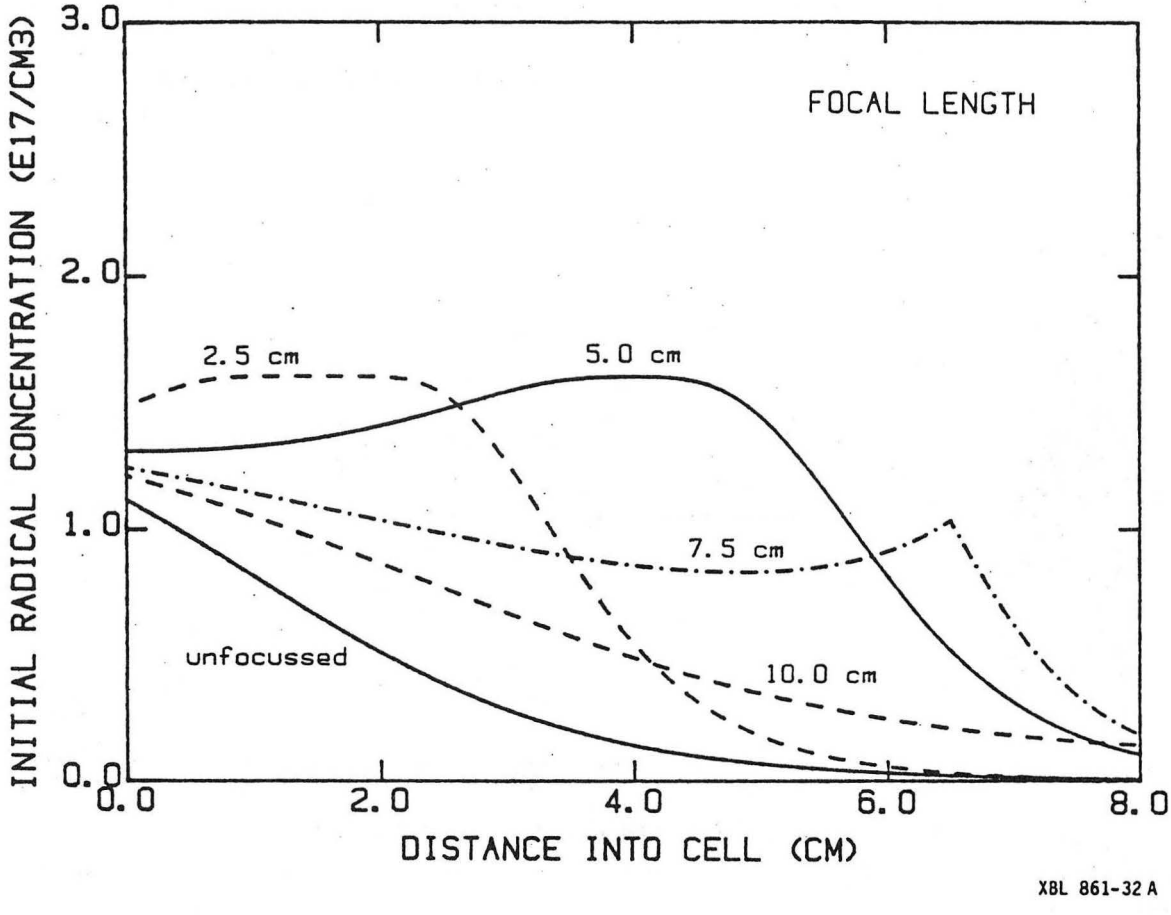
INITIAL RADICAL CONCENTRATION (E17/CM3)
3.0
2.0
1.0
0.0
FOCAL LENGTH
2.5 cm
5.0 cm
7.5 cm
10.0 cm
unfocussed
0.0
2.0
4.0
6.0
8.0
DISTANCE INTO CELL (CM)
XBL 861-32 A

Figure 4.

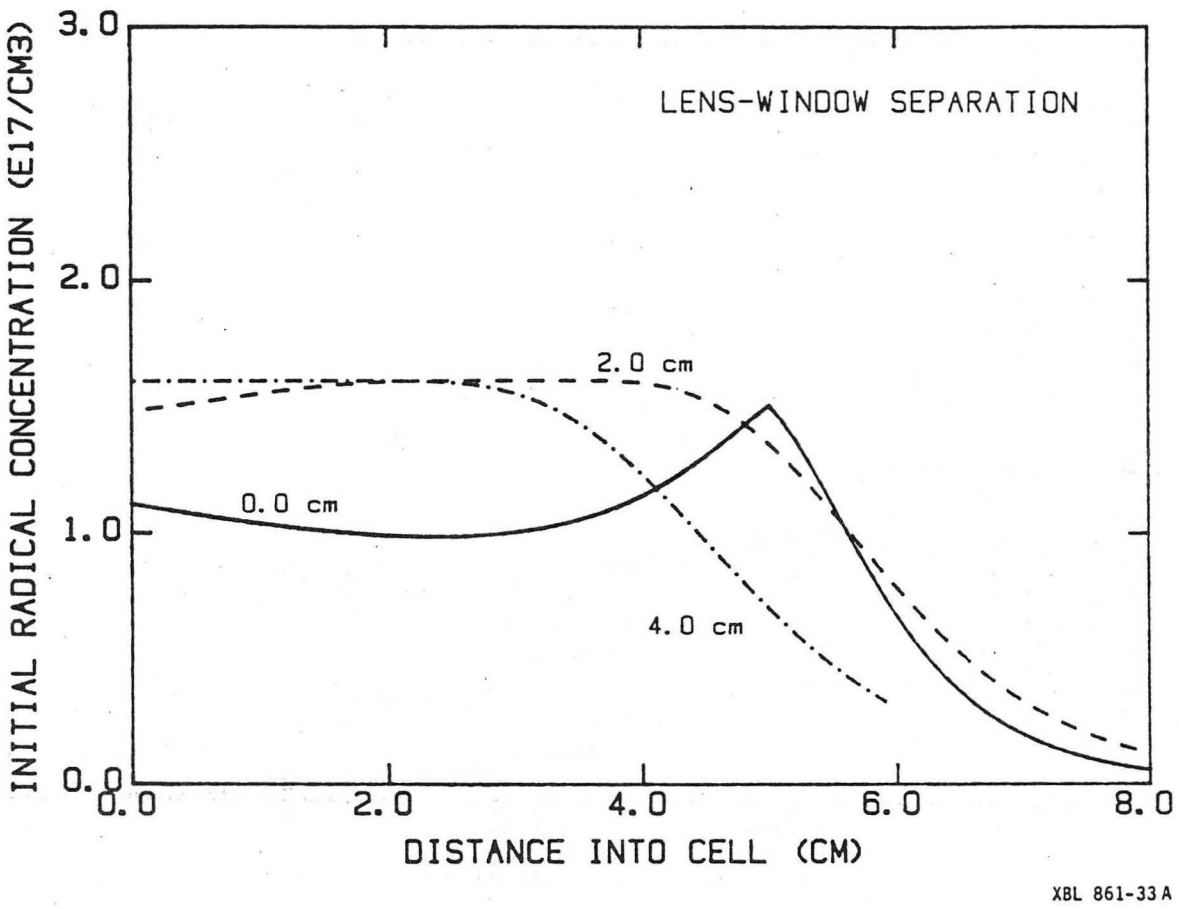
LENS-WINDOW SEPARATION
2.0 cm
0.0 cm
4.0 cm
INITIAL RADICAL CONCENTRATION (E17/CM3)
DISTANCE INTO CELL (CM)
3.0
2.0
1.0
0.0
0.0
2.0
4.0
6.0
8.0
XBL 861-33A

Figure 5.

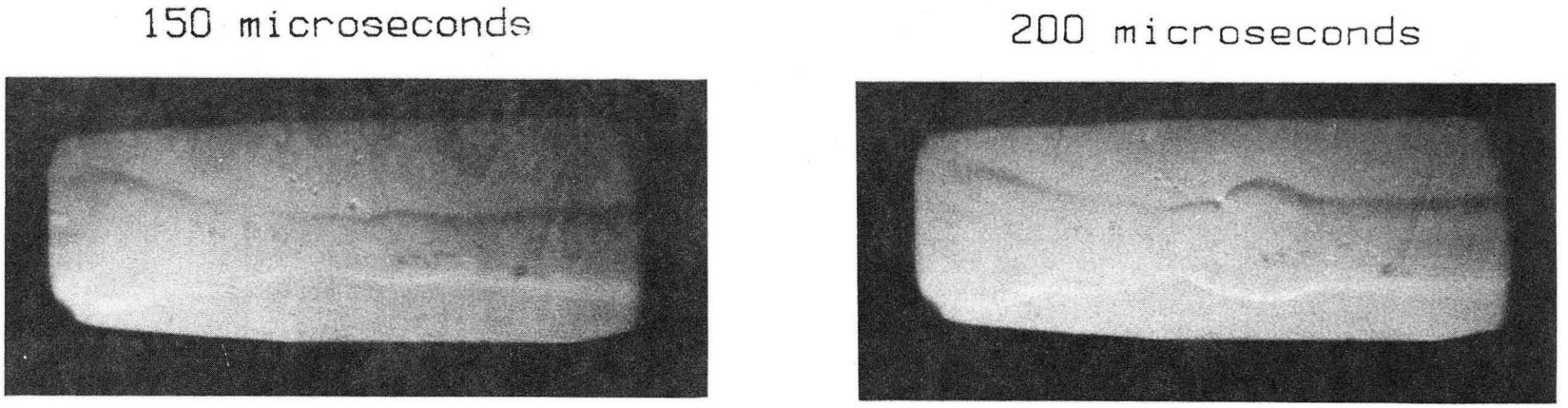
150 microseconds
200 microseconds
IGNITION AT FOCUS
25 microseconds
200 microseconds
IGNITION AT WINDOW
XBB 861-130

Figure 6.

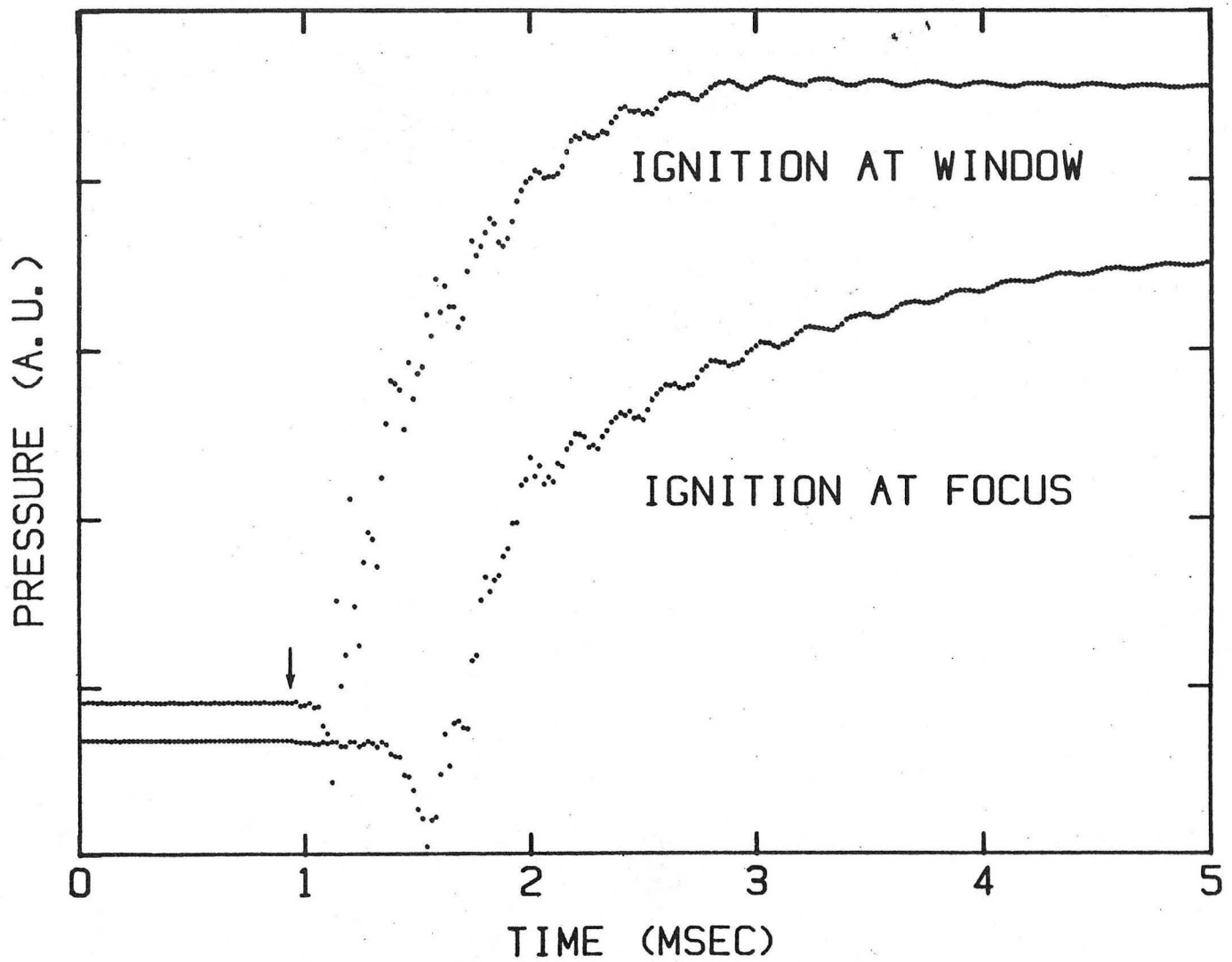

XBL 861-31

Figure 7.

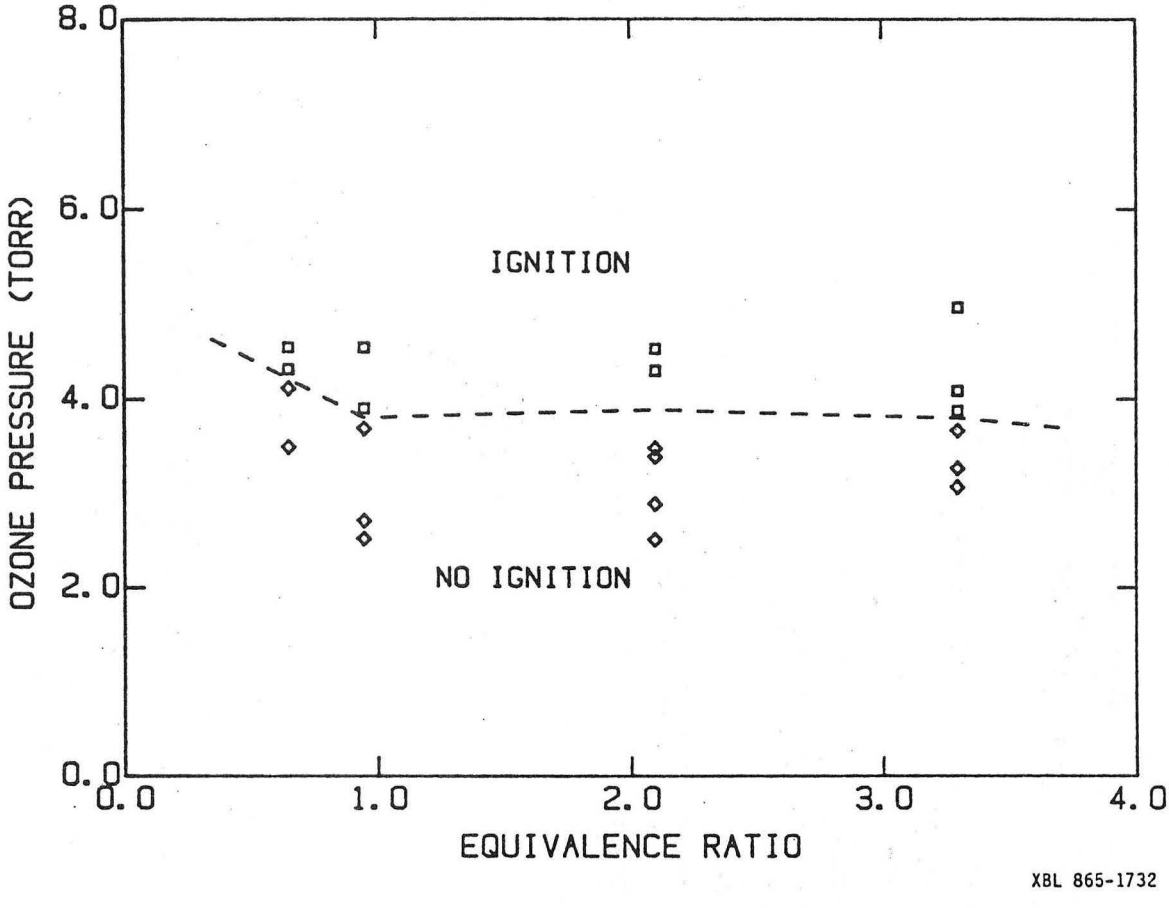
8.0
6.0
4.0
2.0
0.0
OZONE PRESSURE (TORR)
IGNITION
NO IGNITION
0.0
1.0
2.0
3.0
4.0
EQUIVALENCE RATIO
XBL 865-1732

Figure 8.

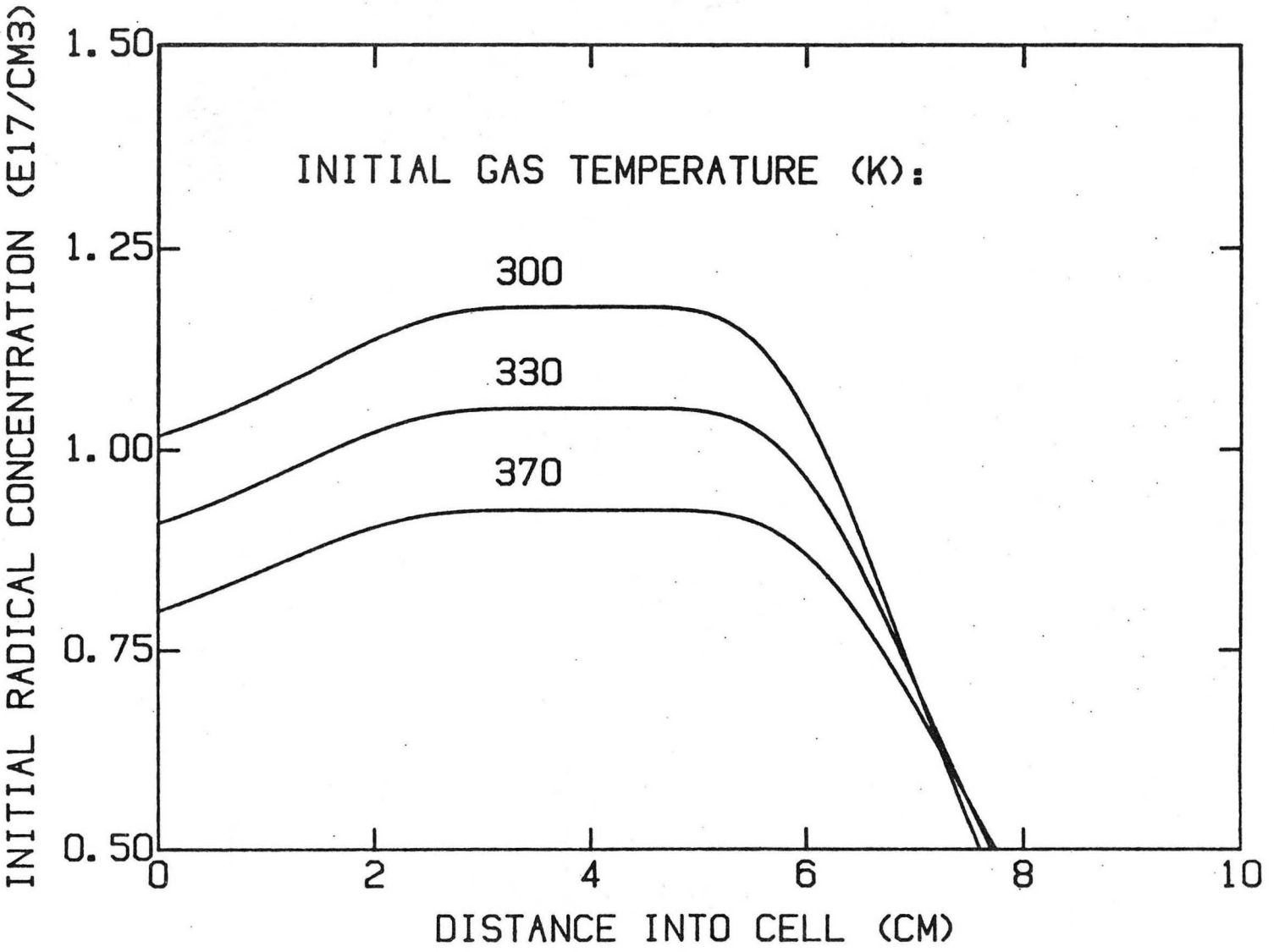

XBL 861-30

Figure 9.

LAWRENCE BERKELEY LABORATORY
TECHNICAL INFORMATION DEPARTMENT
UNIVERSITY OF CALIFORNIA
BERKELEY, CALIFORNIA 94720